Journal of Physical and Theoretical Chemistry
of Islamic Azad University of Iran, 16 (1, 2) 15-28: Spring & Summer 2019
(J. Phys. Theor. Chem. IAU Iran)
ISSN 1735-2126

The NBO, AIM, MEP, thermodynamic and quantum parameters investigations of Pyrrole 2-carboxylic acid molecule adsorption on the pristine and Ni doped B12N12 nano cage

M. Rezaei−Sameti* and F. Zamanian

Department of Applied Chemistry, Faculty of Science, Malayer University, Malayer, 65174, Iran

Received December 2019; Accepted January 2020

ABSTRACT

The main objective of this work is to investigate the adsorption of Pyrrole 2-carboxylic acid (**PCA**) from O, N and C sites on the surface of pristine and Ni doped B12N12 nano cage by using density functional theory (DFT). The results of adsorption energy indicate that the adsorption of **PCA** on the surface of B12N12 and NiB11N12 is exothermic and favorable in thermodynamic viewpoint. Comparison results reveal that adsorption of **PCA** from O head on the surface of B12N12 nano cage is more favorable than other sites, and the recovery time of this site is 2.72×10^{22} s. The change percent of gap energy for adsorption of **PCA** molecule on the surface of pristine B12N12 nano cage is more than Ni doped, thereby the pristine B12N12 nano cage can be a good selected for making **PCA** sensor. The changes Gibbs free energies in water phase ($\Delta\Delta G_{(sol)}$) for adsorption of **PCA** from N and C site of PCA on the surface of B12N12 are negative and spontaneous. The atom in molecule (AIM) and reduced density gradient (RDG) results indicate that the adsorption **PCA** from N and C sites on the surface of B12N12 is strong covalent type, and for other sites is partially covalent bond.

Keywords: Pyrrole 2-carboxylic acid; B12N12; Ni doped; DFT; NBO; AIM

1. INTRODUCTION

Pyrrole compounds and its derivatives are widely known as biologically active compounds and drug products such as anti-inammatory drugs, cholesterol reducing drugs, antibiotics, fungicides, antibacterial, antipsychotic, anxiolytic, antimalarial, antitumor agents, and many more [1−7]. The pyrrole derivatives are found in crude petroleum compound and this material is noxious on metal catalysts utilized in petrochemical industry therefore removal of it from crude petroleum is very important. For this means, the various methods are utilized to adsorb and remove pyrrole compounds from system [8−11]. Qiao et al. [8] investigated the adsorption and thermal reaction of pyrrole on Si(10 0) through X-ray and ultra-violet photoelectron spectroscopy. Bruhn et al. [9] studied the adsorption mechanism of pyrrole on GaAs(001)-c(4-4) surface. Noei et al. [10] examined the electrical sensitivity of boron nitride nanotube toward pyrrole through DFT calculations.

*Corresponding author: mrsameti@gmail.com, mrsameti@malayeru.ac.ir

Shokuhi Rad et al. [11] results reveal that the adsorption energies of pyrrole on Al12N12, Al12P12, B12N12, and B12P12 are negative and exothermic in thermodynamic approach. In current years nano cage of boron nitrides have attracted considerable attention due to their remarkable electrical, chemical and physical properties [12−16]. The experimental attempts [17−18] to observe BN nano cages were performed with electron beam irradiation technology. Fowler et al. [19] theoretically showed that the B12N12 is magic stable BN nano cages, and other studies demonstrate that this nano cage consist entirely of tetragonal and hexagonal BN rings [20−22]. Oku et al. [23] have synthesized these magic cages by using laser desorption time-of flight mass spectrometry. The theoretical study demonstrated that the B12N12 nano cage can be used as chemical sensors and adsorbent for HCN [24], SO_2 [25], NO_2 [26] CO [27], Methylamine [28], CO_2 [29], NO, H_2, N_2 and CH_4 [30], SCN^- [31], phosgene [32], SO_2, O_3 [33], H_2 [34], alkaline metals [35], H_2CO [36], cysteine [37], pyridine [38], methanol [39], phenol [40], caffeine [41], adenine, uracil, cytosine [42] and amphetamine[43]. The results of above works confirm that the BN nano cage is a good candidate to adsorb and detect many compounds.

Following our previous work [44−46], in this project, we decide to investigate the interaction and adsorption of Pyrrole 2-carboxylic acid molecule on surface of pristine and Ni doped B12N12 nano cage. The results of this project may be useful for making adsorbent and detector of **PCA** molecule.

2. COMPUTATIONAL DETAILS

In the current research the interaction of Pyrrole 2-carboxylic acid (**PCA**) on the surface of pristine and Ni doped B12N12 nanocage at different conformations is investigated at the density functional theory (DFT) at Cam-B3LYP/Lanl2dz level of theory by using Gaussian 09 program package [47]. In this study, the maximum force and RMS forces are 4.5×10^{-4}, and 3×10^{-4} whereas maximum displacement and RMS displacement are 1.8×10^{-3} and 1.2×10^{-3}. For study the adsorption of **PCA** molecule on the surface of pristine and Ni doped B12N12 nano cage, we considered different various configurations. The considered various configurations are optimized at the B3LYP/3-21G(d) level of theory, and then the stable structures without imaginary frequency are selected. The selected stable configurations are optimized at Cam-B3LYP/6-31G (d) level of theory again, the optimized structures are shown in the Figs 1 and 2. In this here the (a, c, d) indexes are used to denote the adsorption orientation of **PCA** from O, N and C sites (see Fig. 1). The A and B labels denote to the pristine (B12N12) and Ni doped (NiB11N12). From optimized structures, the adsorption energy, deformation energy, thermodynamic parameters, quantum descriptive, natural bond orbital (NBO), molecular electrostatic potential (MEP), atom in molecule (AIM) and reduced density gradient (RDG) properties of system are calculated and analyzed.

The adsorption energy (E_{ads}) **PCA** on the surface of pristine and Ni doped B12N12 is calculated by Eq. 1:

$$E_{ads} = E_{PCA/B12N12} - E_{PCA} - E_{B12N12} + BSSE \quad (1)$$

where $E_{PCA/B12N12}$ is the total electronic energy of the PCA/B12N12 complex, E_{PCA} and E_{B12N12} is total energy of isolated **PCA** and B12N12 molecule respectively. The BSSE is base set superposition error and for all the complex systems, using counters poise correction method [48].

The quantum descriptive such as HOMO (highest occupied molecular orbital), LUMO (lowest unoccupied molecular orbital), gap energy (E_g) $E_g = E_{LUMO} - E_{HOMO}$, electronic chemical potential (μ) $\mu = 1/2(E_{LUMO} + E_{HOMO})$, global hardness ($\eta$) $\eta = 1/2(E_{LUMO} - E_{HOMO})$, and total charge transfer parameters (ΔN) $\Delta N = -\mu/\eta$ [49−52] are calculated at the above level of theory, and calculated results are tabulated in Table 1.

3. RESULTS AND DISCUSSION

3.1. The geometrical structure and adsorption energies

In this work, at the first step the structures of pristine and Ni doped B12N12 nano cage are optimized at the Cam-B3LYP/6-31G (d) level of density function theory. The geometries of B12N12 are found to be composed of six tetragonal rings and eight hexagonal with Th and S6 symmetry, respectively and the size of studied BN is about 1nm. The bond length of N−B of six tetragonal and eight hexagonal BN ring is 1.509 and 1.438 Å and this result is in agreement with other reports [53−54]. With doping Ni atom, the bond lengths of Ni−B and Ni−N are 1.923 and 1.827 Å and it is more than pristine models.

The optimized results of all adsorption models (Fig. 2) reveal that the bond distance between **PCA** molecule and BN nanocage in the A-a, A-c, A-d, B-a, B-c and B-d models are 1.439, 2.576, 1.810, 1.875, 2.007 and 2.085 Å respectively. The bond angle between **PCA** and nanocage is in range 111.10 to 142.14°.

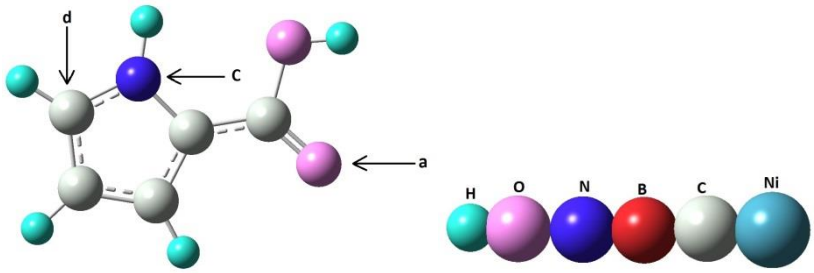

Fig. 1. The orientation Pyrrole 2-carboxylic acid (PCA) molecule for adsorption on B12N12.

Table 1 Adsorption energy (Eads(kcal/mol)), deformation energy of pyrrole 2-carboxylic acid ($E_{def(PCA)}$) , B12N12 (Edef(nano)) , complex B12N12/PCA, binding energy E_{bin} and dipole moment of B12N12/PCA complex for A-a to B-d models.

property	A-a	A-c	A-d	B-a	B-c	B-d
$E_{ads/(kcal/mol)}$	-47.28	-5.20	-4.75	-38.63	-22.35	-28.43
$E_{def(nano)}$ (kcal/mol)	-41.83	-13.38	-13.86	-0.81	-0.91	-1.87
$E_{def(PCA)}$ /(kcal/mol)	-97.50	-10.72	-12.27	-1.24	-4.38	-3.13
μ/Debye	4.54	7.44	7.64	11.22	5.34	6.22
ρ_{NBO}	0.25	0.34	0.35	0.15	0.05	0.07
d (PCA…BN)	1.44	2.58	1.81	1.87	2.01	2.13

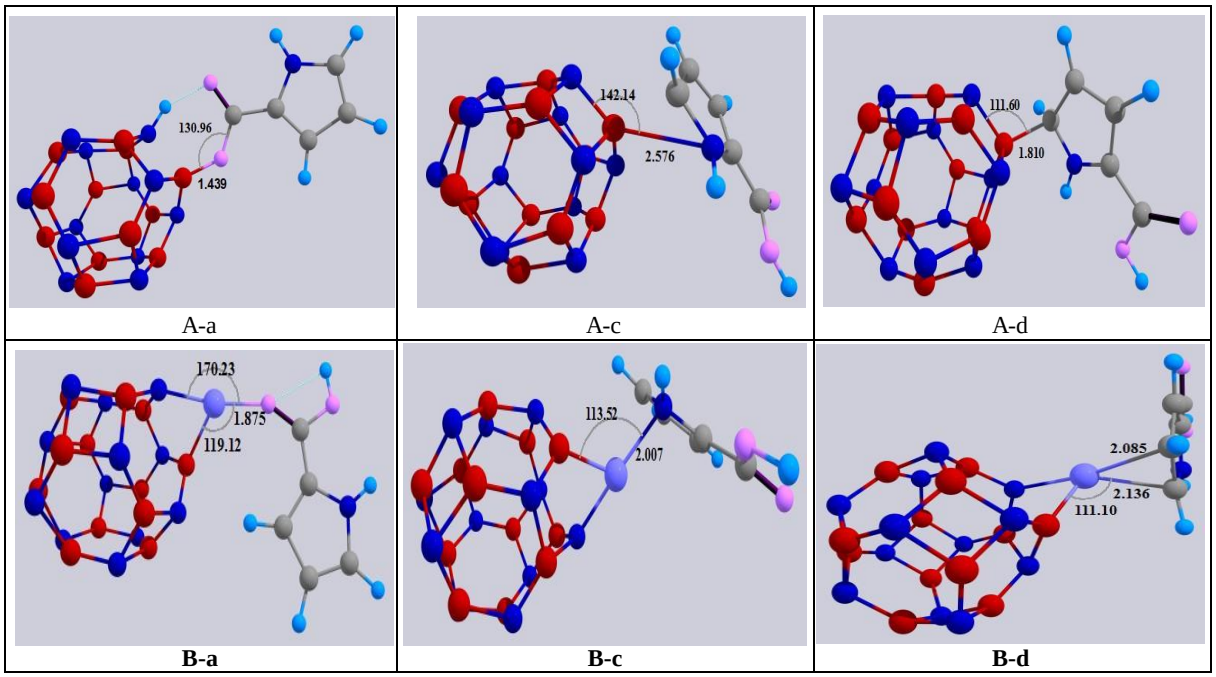

Fig. 2. The geometrical properties for PCA molecule adsorption on the surface of pristine and Ni doped B12N12 for adsorption models: A-a to B-d

The NBO analysis indicate that the charges on B and N atoms of B12N12 nano cage are 1.157 and −1.157 |e| and for Ni doped B12N12 the NBO charges on Ni, B and N atoms of are 0.507, 0.857 and −1.218 |e| respectively. With adsorbing **PCA** on the surface of B12N12 at the A−a and B−a models the NBO charges of B and N atoms are (1.312, −1.280 |e|) and (0.911, −1.245 |e|) respectively. This result reveals that the charge density on the surface of B and N atoms of nano cage increases significantly from original state (see supplementary data).

From NBO analyzes the hybrid of B−N atoms around adsorption position for A-a and B-a models are $sp^{2.27}$ and $sp^{4.34}$ respectively. This result confirms that with doping Ni atom the percentage of P orbital in hybrid of B−N atoms increase and so the bond angle B−N−B near adsorption position from 112.43° in A-a model decrease to 69.78° in B-a model.

Moreover, the NBO charge of **PCA** molecule at the A-a, A-c, A-d, B-a, B-c and B-d models are 0.20, 0.34, 0.35, 0.15, 0.05 and 0.07 |e| respectively (see Table 1). The positive values of NBO charge **PCA** molecule indicate that this molecule has donor electron effect and nano cage has acceptor electron effect, on the other hand with doping Ni atom the NBO charge of **PCA** molecule decease from original state. Therefore, the charges transfer from **PCA** molecule toward BN nano cage decrease.

The dipole moment of the A-a, A-c, A-d, B-a, B-c and B-d models are 4.54, 7.44, 7.64, 11.22, 5.34 and 6.22 Debye (see Table 1). Comparison results reveal that the dipole moment of A-a and B-a is lower and more than other models respectively, due to effect of Ni doped and **PCA** adsorption on the nano cage surface. The adsorption energy (E_{ads}) of the A-a, A-c, A-d, B-a, B-c and B-d models with corrected BSSE are calculated by Eq. 1 and the calculated results are tabulated in Table 1. Close inspection of the obtained results indicate that the E_{ads} of all adsorption models is exothermic and

favorable in thermodynamic view point, and it is in order: A-a (− 47.28 Kcal/mol)> B-a (−38.63 Kcal/mol)> B-d(−28.43 Kcal/mol)> B-c (−22.35 Kcal/mol)> A-c(−5.20 Kcal/mol)> A-d (− 4.75 Kcal/mol).

Comparison results reveal that adsorption of **PCA** from O head on the surface of pristine and Ni doped B12N12 nano cage is more favorable than other site. Except of O site orientation of **PCA**, the adsorption process on the Ni doped B12N12 is more suitable than pristine models.

To further investigating the sensivity of B12N12 nano cage to detect of **PCA** molecule and making sensor device, the recovery time of system is determined by $\tau = \nu_0^{-1} \exp^{(-Ead/kT)}$ equation

(Here, T=298.15 K, k= 0.002 Kcal/mol and $\nu=1\times10^{12}$ s^{-1}). The calculated recovery times for A-a, A-c, A-d, B-a, B-c and B-d are 2.72×10^{22}, 6.12×10^{-9}, 2.88×10^{-9}, 1.36×10^{16}, 1.89×10^{4} and 5.08×10^{8} s respectively. Comparison results demonstrate that the adsorption of **PCA** at the A-c and A-d models is very weak, and these adsorption models are favorable to make a sensitive sensor for **PCA** molecule.

In order to determine the amount of changes in the structures of nanocage and **PCA** molecule, the deformation energy of **PCA** and B12N12 is calculated by Eqs. (2−3).

$$E_{def-B12N12} = E_{B12N12\,pure} - E_{B12N12\,in\,complex} \quad (2)$$

$$E_{def-PCA} = E_{PCA\,pure} - E_{PCA\,in\,complex} \quad (3)$$

where $E_{B12N12\ in\ complex}$ is the total energy of B12N12 in the B12N12/**PCA** complex when **PCA** is absent oneself, and $E_{PCA\ in\ complex}$ is the total energy of **PCA** molecule in the B12N12/**PCA** complex when B12N12 is absent oneself. The calculated results for all adsorption models are listed in Table 1. Based on the calculated results, the deformation energy of **PCA** and B12N12 for all adsorption models is exothermic. It is notable that the amount of deformation energy for A-a model (adsorption of **PCA** from O site on the surface of B12N12) is more negative than other models. For these means, the change of the geometry structure of B12N12 and **PCA** molecule in this model is significantly more than other models.

The thermodynamic parameters such as changes of enthalpies (ΔH), Gibbs free energies (ΔG), entropies (ΔS) and changes Gibbs free energies in water phase ($\Delta\Delta G_{(sol)}$) of the A-a, A-c, A-d, B-a, B-c and B-d models are calculated according to the following Eqs.(2-3):

$$\Delta M = M_{PCA/Nanocluster} - M_{PCA} - M_{nanocluster} \quad M: G, H\ and\ S \quad (4)$$

$$\Delta\Delta G_{(sol)} = \Delta G_{(sol)PCA/Nanocluster} - \Delta G_{(sol)PCA} - \Delta G_{(sol)Nanocluster} \quad (5)$$

Based on the calculated results of Table 2, the values of ΔH, ΔS for all adsorption models are negative. These results reveal that the occurred binding between **PCA** and nanocage is exothermic with reduce entropy. In addition the changes Gibbs free energies (ΔG) in gas phase for A-a, B-a, B-c and B-d models are negative and the adsorption process in these models is spontaneous in thermodynamic approach. The adsorption process in the A-c and A-d models is not spontaneous.

Table 2 The thermodynamic parameters and solvent effect for A-a to B-d models.

	ΔH(Kcal/mol)	**ΔG(Kcal/mol)**	**ΔS(Cal/mol-K)**	**$\Delta G_{(SOL)}$(Kcal/mol)**
A-a	-45.98	-33.75	-40.99	36.12
A-c	-4.24	7.86	-40.60	-10.20
A-d	-3.81	8.46	-41.17	-10.88
B-a	-37.01	-25.20	-39.63	42.99
B-c	-21.46	-10.94	-35.29	27.3
B-d	-27.50	-16.83	-35.79	33.74

Whereas the changes Gibbs free energies in water phase ($\Delta\Delta G_{(sol)}$) for A-c and A-d models are negative and spontaneous. The $\Delta\Delta G_{(sol)}$ values for other models are positive. These results demonstrate that the adsorption of **PCA** on the surface of B12N12 and NiB12N12 at the A-a, B-a, B-c and B-d models is not favorable in thermodynamic approach.

3.2. The HOMO- LUMO and quantum descriptive

In order to better comprehend the electrical properties of adsorption **PCA** on the surface of pristine and Ni doped B12N12 nanocage the highest occupied molecular orbital (HOMO) and the lowest unoccupied molecular orbital (LUMO) are calculated and the results are depicted in Fig. 3.

The HOMO orbital density in A-a, A-c and A-d is mostly localized on the surface of nanocage,

whereas the density of LUMO orbital is localized around **PCA** molecule. With doping Ni atom the HOMO orbital density in the B-a, B-c and B-d models is located around adsorption position on surface nanocage and **PCA** molecule, whereas the LUMO orbital density is localized entirely around **PCA** surface. The HOMO and LUMO energies of pristine B12N12 nanocage are −7.87 and −1.93 eV, with doping Ni atom the HOMO and LUMO energies significantly alter to −6.52 and −3.12 eV, therefore the gap energy decrease from 5.94 to 3.40 eV (See Table S1 in supplementary data). Upon adsorption of **PCA** on the surface of pristine B12N12 the gap energy decease significantly from 5.94 eV to 4.88 eV (A-a model), 3.43 eV (A-c model) and 3.32 eV (A-d model) eV (Table 2). These results demonstrate that the conductivity of pristine nanocage increase upon **PCA** adsorption and this property is suitable for making nano sensor. On the other hand, with doping Ni atom the gap energy of nanocage change from 3.40 eV to 3.03 eV (B-a model), 3.55 eV(B-c model) and 3.74 eV(B-d model). The incensement in gap energy of B-c and B-d caused that the conductivity of nano cage decrease from original values (Table 2). The most change percent of gap energy $\left(\%\Delta E_g = \frac{(E_{g\,(nanocluster/PCAcomplex)} - E_{g\,(nanocluster)})}{E_{g\,(nanocluster)}} \times 100\right)$ is observed in the A-d model (− 44.10 %) and the lowest change is observed in the B-c model (4.41%). Comparison results indicate that the change percent of gap energy after adsorbing **PCA** molecule on the surface of pristine B12N12 nanocage is more than Ni doped; thereupon the pristine B12N12 nanocage is more favorable than NiB11N12 nanocage for making **PCA** sensor. The density of states (DOS) are also calculated for A-a, A-c, A-d, B-a, B-c and B-d adsorption models in confine energy of −15 to 5 eV, shown in Fig. 4. The number of DOS peaks on the occupied orbital region for B12N12 and NiB11N12 nanocage are 9 and 12 respectively, and the number of DOS peaks on the unoccupied orbital region for B12N12 and NiB11N12 nanocage are 9 and 11 respectively. Upon adsorbing **PCA** molecule on the surface of B12N12 and NiB11N12 nanocage, the number of DOS peaks increase, this property supported the changes of gap energy results. From HOMO and LUMO levels energy the electronic chemical potential (μ), global hardness (η) and total charge transfer parameters (ΔN) are calculated and the results are listed in Table 3. The global hardness illustrate the reactivity and stability of a molecule or complex. The global hardness of **PCA**, B12N12 and NiB11N12 are 2.56, 2.97 and 1.70 eV respectively (Table S1 supplementary data). The B12N12 nanocage is relatively harder than NiB11N12 and **PCA** molecule. It is interesting that the global hardness A-

a, A-c, A-d and B-a models are lower than pure nanocage. Since global hardness is a measure of stability of a system towards deformation in the presence of electrical field; and so, the stability of system under electrical field with adsorbing **PCA** on the surface of pristine B12N12 decrease significantly from pure state. The chemical potential of **PCA**, B12N12 and NiB11N12 are −3.99, −4.90 and −4.82 eV respectively. Comparison results indicate that the chemical potential of A-a (−4.38 eV), B-a (−4.19 eV), B-c (−4.39 eV) and B-d (−4.45 eV) is more than before adsorption states and so the reactivity of nanocage is more than before adsorption states. On the other hand, the chemical potential of **PCA** molecule is larger than B12N12 and NiB11N12; thereby the charge transfer occurs from **PCA** molecule toward nanocage. The positive values of ΔN (total charge transfer) and $\rho_{(NBO)}$ confirm that the charge transfer occur from **PCA** molecule toward nanocage (Tables 1 and 2). For this means, the most negative charge is located around nanocage. The values of ΔN and $\rho_{(NBO)}$ for A-c and A-d models are larger than other studied models, and this result is in agreement with density of HOMO and LUMO orbital in Fig. 4.

3.3 The natural bond orbital (NBO) and molecular electrostatic potential (MEP)

One of the efficient and helpful methods to investigate the interaction between two compounds and charge transfer between the atoms during the reaction is natural bond orbital [55]. NBO includes information such as donor (i), acceptor (j) occupancy, $E^{(2)}$(stabilization energy), $\varepsilon_i - \varepsilon_j$ (energy difference between donor and acceptor i and j NBO orbitals), F_{ij} (the Fock matrix element between i and j NBO orbitals) , that $E^{(2)}$ is calculated from the Eq. 4:

$$E^{(2)} = q_i \frac{F_{ij}^2}{\varepsilon_j - \varepsilon_i} \qquad (6)$$

where q_i is donor orbital occupancy, ε_i and ε_j are orbital energies and F_{ij} is the off−diagonal NBO Fock matrix element. NBO analysis for **PCA** molecule and pristine, Ni-doped B12N12 nano cage are done using DFT/B3LYP method and Lanl2dz basis set, the calculated results between selected donor and acceptor orbital of A-a, A-c, A-d, B-a, B-c and B-d models are given in Table 4 and for all system are given in Table S3 in supplementary data. According to calculated results of Table 4 the most interaction between **PCA** and nano cage occur in $\sigma N_1 - B_1 \rightarrow \sigma^* N_8 - B_2$ for A-d model with $E^{(2)}$=9.30 Kcal/mol. Which indicates the strongest charge transfer interaction is responsible between **PCA** molecule and nanocage in this model. The least interaction occurs in $\sigma N_2 - B_1 \rightarrow \sigma^* N_5 - B_4$ for A-a model with $E^{(2)}$= 1.82 Kcal/mol.

Table 3 Quantum parameters for adsorption of pyrrole 2-carboxylic acid (PCA) on the surface of pristine (A model) and Ni (B model) functionalized B12N12 for A-a to B-d models.

Model	A-a	A-c	A-d	B-a	B-c	B-d
$E_{(HOMO)}$/ /eV	-6.81	-7.06	-7.04	-5.71	-6.17	-6.32
$E_{(LUMO)}$ /eV	-1.93	-3.63	-3.72	-2.68	-2.62	-2.58
$E_{(gap)}$ /eV	4.88	3.43	3.32	3.03	3.55	3.74
μ/eV	-4.38	-5.34	-5.38	-4.19	-4.39	-4.45
η/$(eV)^{-1}$	2.45	1.71	1.66	1.51	1.77	1.87
ΔN	1.78	3.12	3.24	2.77	2.48	2.37
%ΔE_{gap}	-17.84	-42.25	-44.10	-10.88	4.41	10.00

Table 4 The second-order perturbation energies (**2**) [donor (*i*) → acceptor (*j*)] for A-a to B-d models.

Structure	Donor(i)	→	Acceptor(j)	E(2) (Kcal/mol)	E(j)-E(i) (a.u.)	F(i.j) (a.u.)
A-a	σ N1-B1	→	N3-B3* σ	3.89	0.93	0.054
	N2-B1 σ	→	N7-B6* σ	5.16	0.78	0.058
	N2-B1 σ	→	N5-B4* σ	1.82	0.81	0.035
A-c	N1-B1σ	→	N3-B3* σ	4.35	0.92	0.057
	N1-B1σ	→	N7-B6* σ	4.19	0.93	0.056
	N1-B1σ	→	σ* N5-B4	2.80	0.94	0.046
A-d	N1-B1σ	→	N3-B3σ*	4.25	0.92	0.056
	N1-B1σ	→	N8-B2σ*	9.30	0.99	0.086
	N1-B1σ	→	N1-B2σ*	2.85	0.94	0.047
B-a	σN1-NI25	→	σ*N8-B2	5.57	0.81	0.062
	σN2-B1	→	σ*N7-B6	4.47	0.97	0.059
	σN2-B1	→	σ*N5-B4	2.78	0.93	0.045
B-c	σ B1-NI25	→	σ*N8-B2	1.87	0.70	0.033
	σN2-B1	→	σ*N7-B6	4.46	0.97	0.059
	σN2-B1	→	σ*N5-B4	2.86	0.94	0.046
B-d	σB1-NI25	→	σ*N8-B2	2.02	0.68	0.034
	σB1-NI25	→	σ*N7-B6	2.34	0.65	0.035
	σB1-NI25	→	σ*N5-B4	3.97	0.72	0.049

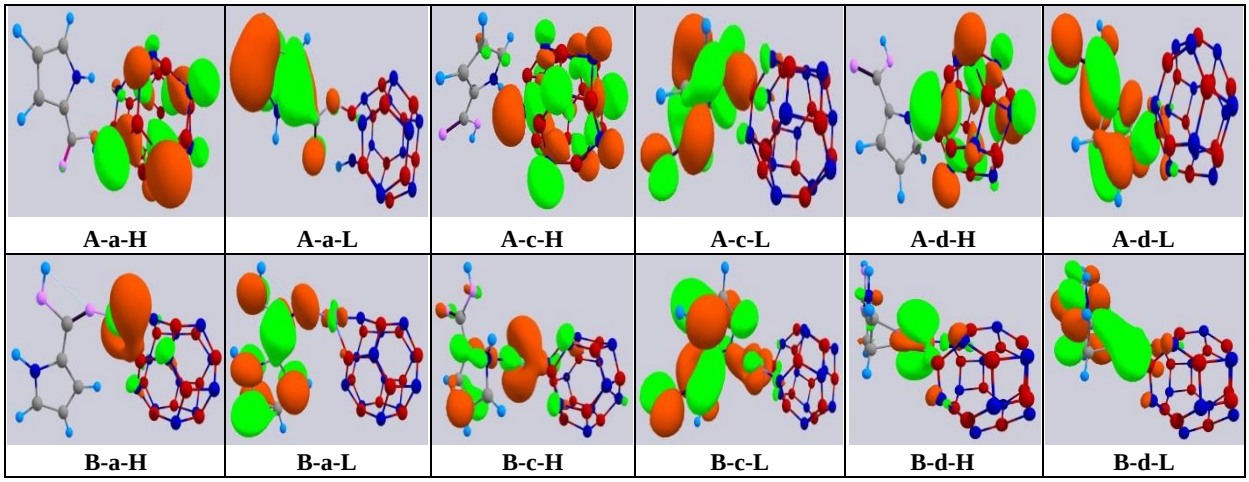

Fig. 3 The HOMO-LUMO for PCA molecule adsorption on the surface of pristine and Ni doped B12N12 for adsorption models: A-a to B-d

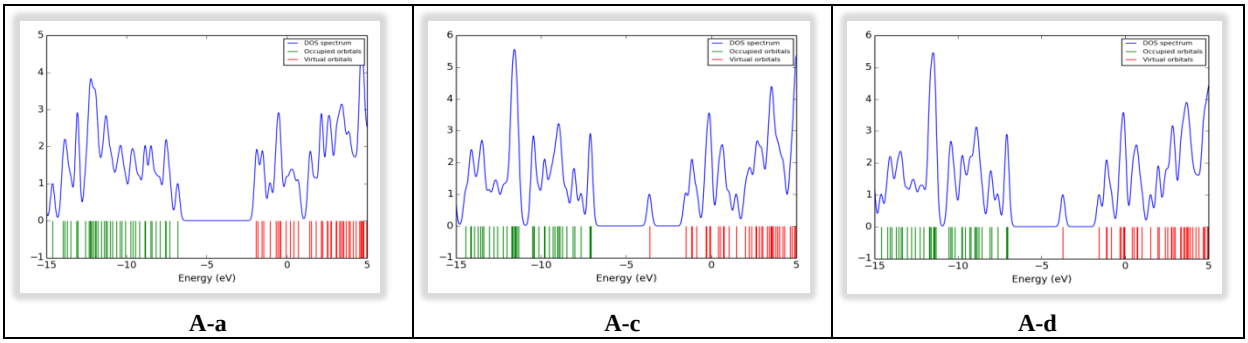

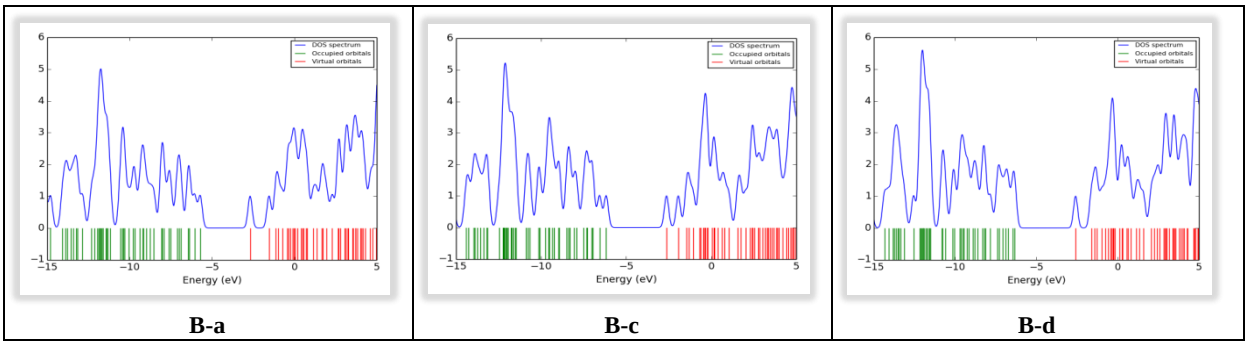

Fig. 4 The DOS plots for PCA molecule adsorption on the surface of pristine and Ni doped B12N12 for adsorption models: A-a to B-d

The calculated results indicate that the $E^{(2)}$ values of A-a, A-c and A-d models (adsorption of **PCA** on the surface of B12N12 nano cage) are relatively larger than Ni doped models. Thereby the charge transfer between **PCA** molecule and pristine B12N12 is more than NiB11N12, and this result agree with the quantum parameters too.

The molecular electrostatic potential (MEP) maps is used to identify the electronic sites of positive and negative electrostatic potential for nucleophilic and electrophilic attack [56]. In the MEP maps, the difference of the electrostatic potential at the surface of molecule is represented different color. The negative regions (red color) with the high electron density related to electrophilic reactivity, the positive regions (blue color) with the low electron density ones to nucleophilic reactivity. The calculated MEP maps are shown in Fig. 5. According to maps of Fig 5, the surface of nanocage with red color has the highest electron density and surface of **PCA** with blue color has the lowest electron density. These results confirm that the surface of nanocage with negative charge is suitable for electrophilic attack, and surface of **PCA** molecule with positive charge is favorable for nucleophilic attack, and these results agree the NBO charge and HOMO- LUMO maps.

3.4 Atom in molecule (AIM) and reduced density gradient (RDG)

By using atom in molecule (AIM) method, we can obtain additional information on the electronic structure at the bond critical points (BCP). BCPs are certain points where the first derivative of electron density vanishes i.e. $\nabla^2\rho = 0$ and it being a saddle point of electron density between two atoms forming a chemical bond [57].
The electron densities (ρ), Laplacian of electron densities ($\nabla^2\rho$), the potential energy (V_{BCP}), the total electronic energy (H_{BCP}), and the kinetic energy (G_{BCP}) at bond critical point (BCP) are calculated using AIMALL program [58]. The results of AIM properties at bond critical point are shown in Fig 6 and are given in Table 5. According to Bader theory the positive values of $\nabla^2\rho$ and H values denote the weak covalent interactions (strong electrostatic bond), negative value of $\nabla^2\rho$ and H values refer to strong interaction (strong covalent bond), and medium strength ($\nabla^2\rho>0$ and $H<0$) is defined as partially covalent bond.

Based on the calculated results of Table 5, the values of $\nabla^2\rho$ and H for A-c and A-d models are negative, denoting strong covalent bond between **PCA** and B12N12 nanocage. Whereas, for A-a , B-a, B-c and B-d models, the values of $\nabla^2\rho$ and H are positive and negative respectively, representing a partially covalent bond

interaction between **PCA** molecule and nanocage.

In order to understand the real space weak interaction between **PCA** molecule and pristine and Ni doped B12N12 nanocage, the reduced density gradient (RDG) parameter based on the electron density and their derivatives is calculated by following equation[58].

$$RDG(r) = \frac{1}{2(3\pi^2)^{1/3}} \frac{|\nabla\rho(r)|}{\rho(r)^{4/3}} \quad (7)$$

The weak interactions are isolated with the regions about low reduced density gradient value and the low electron density values. In this work, the RDG plots for all adsorption models in a completely wide range of interactions types are calculated plots and results are shown in Fig. 7. In the RDG plots red color circle shows the bonded (hydrogen or electrostatic bond) (λ_2<0) interactions, green circle implies low electron density(λ_2=0) , corresponding to Van der walls interactions and blue color circle denotes nonbonding (λ_2>0) interactions. The survey of Fig 7, displays that in the all adsorption models more electron density localized in λ_2<0 regions and the attractive interactions is increase. This result confirms the exothermic values of adsorption energy and electrostatic type adsorption between PCA and BN nano cage.

Table 5 The topological parameters of AIM method for A-a to B-d adsorption models

	ρ	$\nabla^2\rho$	G	H	V	$\|V/G\|$
A-a	0.1539	0.5832	0.2587	-0.1129	-0.3717	1.4368
A-c	0.0924	-0.0812	0.0411	-0.0614	-0.1025	2.4939
A-d	0.0935	-0.0774	0.0466	-0.0660	-0.1126	2.4166
B-a	0.0878	0.6866	0.1821	-0.0105	-0.1926	1.0576
B-c	0.0782	0.4192	0.1158	-0.0111	-0.1269	1.0958
B-d	0.1029	0.0254	0.0474	-0.0411	-0.0884	1.8649

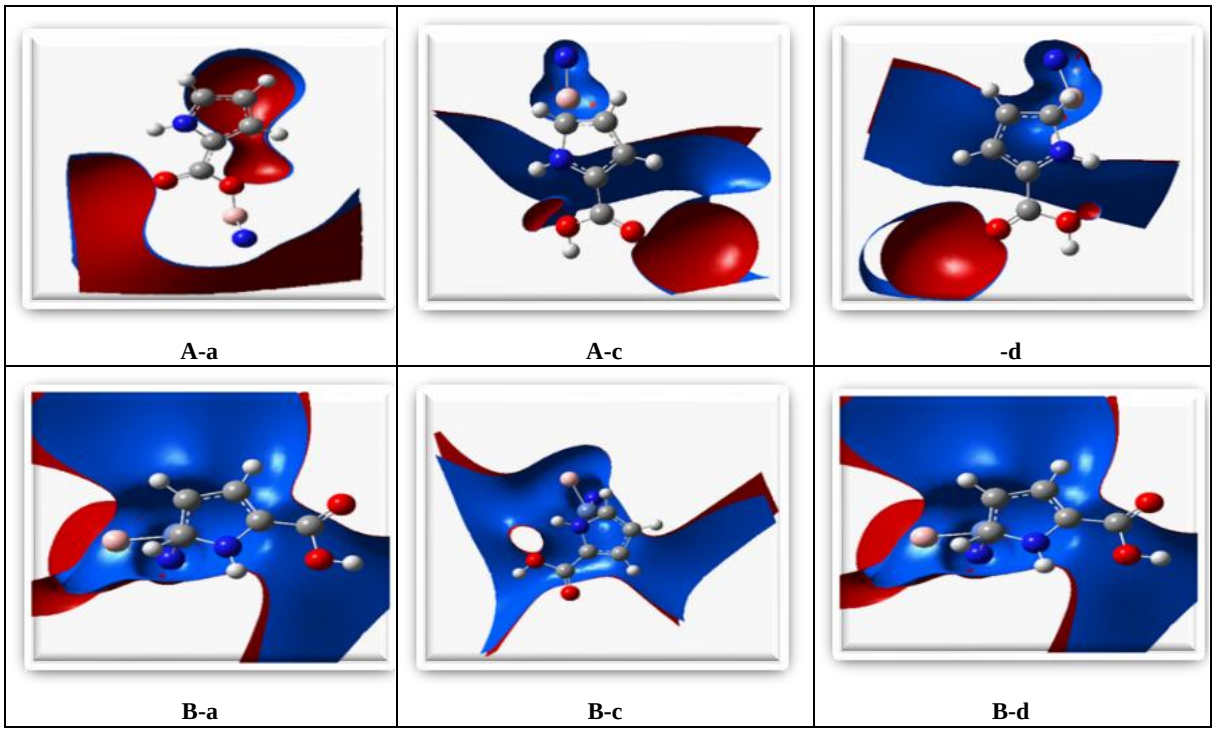

Fig. 5 The MEP for PCA molecule adsorption on the surface of pristine and Ni doped B12N12 for adsorption models: A-a to B-d.

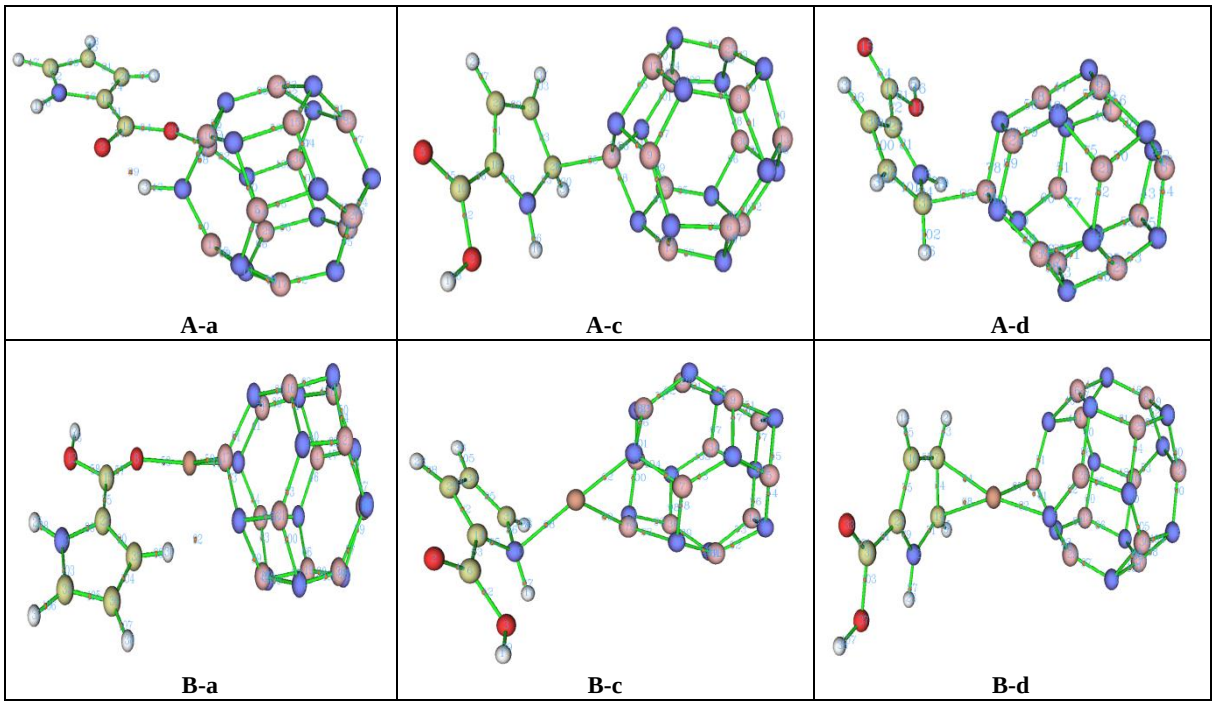

Fig. 6 The AIM plots for PCA molecule adsorption on the surface of pristine and Ni doped B12N12 for adsorption models: A-a to B-d

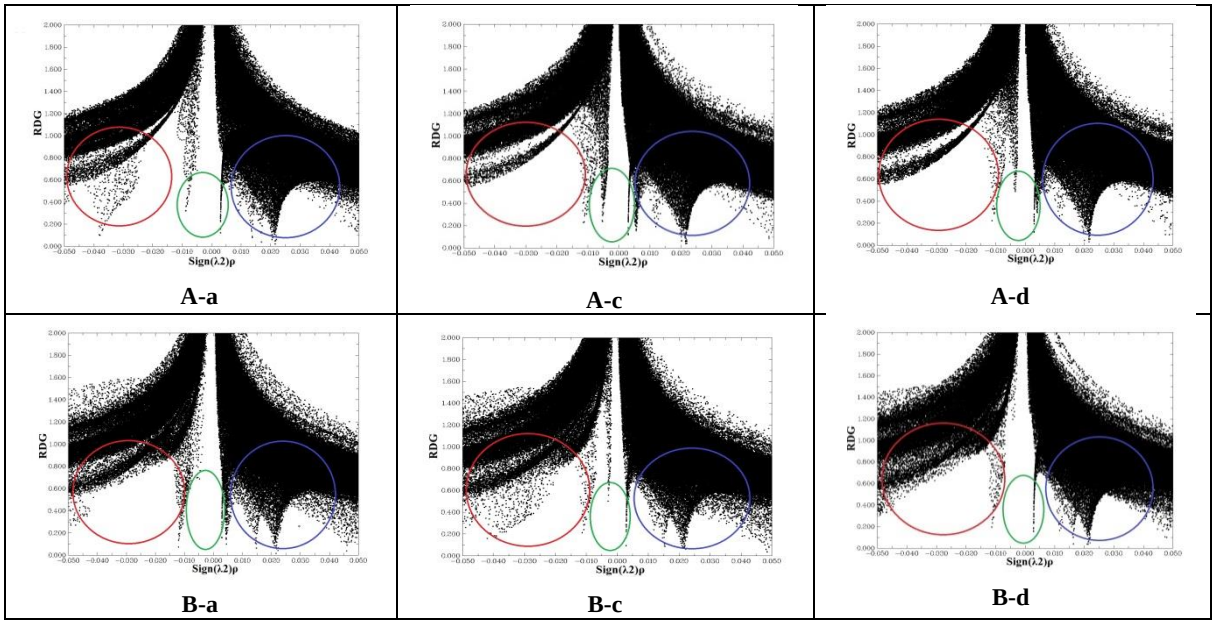

Fig. 7 The RDG for PCA molecule adsorption on the surface of pristine and Ni doped B12N12 for adsorption models: A-a to B-d

4. CONCLUSIONS

In this study, by using DFT method, the adsorption and interaction of the **PCA** molecule on the surface B12N12 and NiB11N12 nano cage is investigated at the cam-B3LYP/6-31G(d) level of theory. The adsorption energy (E_{ads}) values of the A-a, A-c, A-d, B-a, B-c and B-d models are negative and exothermic. The calculated gap energy of **PCA** &B12N12 complex

reduces significantly from original values and so the conductivity of system increases from original state, this property is suitable for making nano sensor. Comparisons of the calculated recovery time of studied systems demonstrate that the adsorption of **PCA** on the surface of nanocage at the A-c and A-d models is very weak, and these adsorption models are favorable to make a sensitive sensor for **PCA** molecule. The changes of Gibbs free energy and enthalpy values for the A-a, B-a, B-c and B-d models are negative and these results reveal that the adsorption process of all studied models are favorable and spontaneous, whereas the changes of Gibbs free energy in present of water solvent is positive and unspontaneous in thermodynamic approach. The calculated results confirm that the Ni doped B12N12 is a good candidate to making sensor and absorber of **PCA** molecule.

ACKNOWLEDGMENT

The author thanks the Computational information center of Malayer University for providing the necessary facilities to carry out the research.

SUPPLEMENTARY DATA

Tables S1− S3 and Figures S1− S8 are given in supplementary data.

REFERENCES

[1] V. Bhardwaj, D. Gumber, V. Abbot, S. Dhiman, and P. Sharma, RSC Adv 5 (2015) 15233– 15266.
[2] W. W. Wilkerson, R. A. Copeland, M. Covington and J. M. Trzaskos, J. Med. Chem. 38 (1995) 3895–3901.
[3] R. P. Wurz and A. B. Charette, Org. Lett. 7 (2005) 2313–2316.
[4] H. Lee, J. Lee, S. Lee, Y. Shin, W. Jung, J.-H. Kim, K. Park, K. Kim, H. S. Cho and S. Ro, Bio org. Med. Chem. Lett. 11 (2001) 3069–3072.
[5] C. Piliego, T. W. Holcombe, J. D. Douglas, C. H. Woo, P. M. Beaujuge and J. M. Fr´echet, J. Am. Chem. Soc. 132 (2010) 7595–7597.
[6] A. R. Katritzky, P. Barczynski, G. Musumarra, D. Pisano and M. Szafran, J. Am. Chem. Soc., 111(1989) 7–15.
[7] D. Yogesh ,M. Mane Santosh,O. Surwase Dhanraj, P. Biradar Yuvraj, H. Sarnikar Balaji, S. Jawle Vishnu, and C. Shinde Bhimrao, Khade, J. Hetrocyclic Chem. 54 (2017) 2627–2634.
[8] M. H. Qiao, F. Tao, Y. Cao, and G.Q. Xu, Surf. Sci. 544 (2003) 285–294.
[9] T. Bruhn, B.O. Fimland, N. Esser, and P. Vogt, Phys. Rev. B. 85 (2012) 075322.
[10] M. Noei, A.H. Jafargholi, and A.A. Salari, Int. J. New Chem. 1 (2014) 18–26.
[11] A. Shokuhi Rad, and K. Ayub, Vacuum 131 (2016) 135–141.
[12] R. T. Paine, and C.K. Narula, Chem. Rev. 90 (1990) 73–91.
[13] H. S. Wu, F.Q. Zhang, X. H. Xu, C.J. Zhang, and H. Jiao, J. Phys. Chem. A. 107 (2003) 204–209.
[14] H. Y. Zhu, T.G. Schmalz, and D. J. Klein, Int. J. Quant. Chem. 63 (1997) 393–401.
[15] D. Goldberg, Y. Bando, O. Stepahan, and K. Kurashima, Appl. Phys. Lett. 73 (1998) 2441–2443.
[16] Q. Wang, Q. Sun, P. Jena, and Y. Kawazoe, ACS Nano 3(2009) 621–626.
[17] O. Stephan, Y. Bando, A. Loiseau, F. Willaime, N. Shramchenko, T. Tamiya, and T. Sato, Appl. Phys. A: Mater. Sci. Process. 67 (1998) 107–111.
[18] D. Golberg, Y. Bando, O. Stephan, and K. Kurashima, Appl. Phys. Lett. 73 (1998) 2441–2443.

[19] G. Seifert, R. Fowler, D. Mitchell, D. Porezag, and T. Frauenheim, Chem. Phys. Lett. 268 (1997) 352–358.
[20] D. Strout, J. Phys. Chem. A. 104 (2000) 3364–3366.
[21] D. Strout, J. Phys. Chem. A. 105 (2001) 261–263.
[22] X.Y. Cui, B.S. Yang, and H.S. Wu, Comput. Theo. Chem. 941 (2010) 144–149.
[23] T. Oku, A. Nishiwaki, and I. Narita, Physica B. 351 (2004) 184–190.
[24] M.T. Baei, Comput. Theo. Chem. 1024 (2013) 28–33.
[25] M. Noei,Vacuum**.** 135 (2017) 44–49.
[26] J. Beheshtian, M. Kamfiroozi, Z. Bagheri, and A.A. Peyghan, Chin. J. Chem. Phys. 25 (2012) 60–64.
[27] J. Beheshtian, Z. Bagheri, M. Kamfiroozi, and A. Ahmadi, Microelectron. J. 42 (2011) 1400–1403.
[28] M.D. Esrafili, and R. Nurazar, Surf. Sci. 626 (2014) 44–48.
[29] M. T. Baei, Z. Bagheri, and A. A. Peyghan, Bull. Korean Chem. Soc. 33 (2012) 3338–3342.
[30] J. Beheshtian, A. A. Peyghan, Z. Bagheri, and M. Kamfiroozi, Struct. Chem. 23(2012) 1567–1572.
[31] A. Soltani, M.T. Baei, E.T. Lemeski, and A.A. Pahlevani, Superlatt. Microstruct. 75 (2014) 716–724.
[32] [32] E. Shakerzadeh, E. Khodayar, and S. Noorizadeh,. Comp. Mat. Sci. 118 (2016) 155–171.
[33] A. Shokuhi Rad, and K. Ayub, Solid State Sci. 69 (2017) 22–30.
[34] A.S. Rad, and K. Ayub, Int. J. Hydrogen Energy. 41 (2016) 22182–22191.
[35] J. Beheshtian, M.B. Tabar, Z. Bagheri, and A.A. Peyghan, J. Mol. Model. 19 (2013) 1445–1450.
[36] E. Shakerzadeh, Physica E. 78 (2016) 1–9.
[37] M. Bezi Javan, A. Soltani, E. Tazikeh Lemeski, A. Ahmadi, Sahar, and M. Rad, Superlattices Microstr. 100 (2016) 24–37.
[38] M.T. Baei, Superlattices Microstruct. 58 (2013) 31–37.
[39] M.D. Esrafili, and R. Nurazar, Superlattices Microstruct. 67 (2014) 54–60.
[40] A. Soltani, M.T. Baei, M. Ramezani Taghartapeh, E. Tazikeh Lemeski, and S. Shojaee, Struct. Chem. 26 (2015) 685–693.
[41] A. Soltani, M.T. Baei, E. Tazikeh Lemeski, and M. Shahini, Superlattic. Microstruct. 76 (2014) 315–325.
[42] M.T. Baei, M. Ramezani Taghartapeh, and E. Tazikeh Lemeski, Phys. B. 444 (2014) 6–13.
[43] A. Bahrami, S. Seidi, T. Baheri, and M. Aghamohammadi, Superlat. Microstruct. 64 (2013) 265–273.
[44] M. Rezaei−Sameti, and S. Baranipour, J. Phys.Theo. Chem. 14 (2017) 211–228.
[45] M. Rezaei−Sameti, and P. Zarei, Adsorption. 24 (2018)757–776 .
[46] M. Rezaei−Sameti, and S. Yaghoobi, Comp. Condens Mat, 3(2015) 21–29.
[47] M. J. Frisch, et. al. Gaussian 09, Revision D.01, Gaussian, Inc., Wallingford CT (2009).
[48] F. Tournus, and J.C. Charlier, Phys. Rev. B 71(2005) 165421.
[49] R.G. Parr, R. A. Donnelly, M. Levy, and W. E. Palke, J. Chem. Phys. 68 (1978) 3801–3807.
[50] R. G. Parr, and W. Yang, J. Am. Chem. Soc. 106 (1987) 4049–4050.
[51] [51] M. Gorbunova, I. Shein, Y. N. Makurin,V. Ivanovskaya,V. Kijko, and A. Ivanovskii, Physica E. 41 (2008) 164-168.
[52] J. He, K. Wu, R. Sa, Q. Li, and Y. Wei, Appl. phys. let. 97(2010) 051901.

[53] A.V. Pokropivny, Diam, Relat. Mater. 15 (2006) 1492–1495.
[54] M. T. Baei, M. Ramezani Taghartapeh, E. Tazikeh Lemeski, and A. Soltani, Physica B. 444 (2014) 6–13.
[55] A. Nataraj, V. Balachandran, and T. Karthick, J. Mol. Struct. 1022 (2012) 94–108.
[56] M. Sheikhi, and D. Sheikh, Rev, Roum. Chim. 59(2014) 761–767.
[57] R. F. W. Bader, Oxford University Press, Oxford, U.K. (1990).
[58] F. Biegler−Konig, University of Applied Sciences, Bielefeld (2001).